The EMBO Journal Vol.18 No.1 pp.145–155, 1999

Activation of the *Drosophila* C3G leads to cell fate changes and overproliferation during development, mediated by the RAS–MAPK pathway and RAP1

Satoshi Ishimaru, Rosemary Williams, Elizabeth Clark[1], Hidesaburo Hanafusa and Ulrike Gaul[1,2]

Laboratory of Molecular Oncology and [1]Laboratory of Developmental Neurogenetics, The Rockefeller University, 1230 York Avenue, New York, NY 10021, USA

[2]Corresponding author
e-mail: gaul@rockvax.rockefeller.edu

H.Hanafusa and U.Gaul contributed equally to this work

The cellular signal transduction pathways by which C3G, a RAS family guanine nucleotide exchange factor, mediates v-*crk* transformation are not well understood. Here we report the identification of *Drosophila* C3G, which, like its human cognate, specifically binds to CRK but not DRK/GRB2 adaptor molecules. During *Drosophila* development, constitutive membrane binding of C3G, which also occurs during v-*crk* transformation, results in cell fate changes and overproliferation, mimicking overactivity of the RAS–MAPK pathway. The effects of C3G overactivity can be suppressed by reducing the gene dose of components of the RAS–MAPK pathway and of RAP1. These findings provide the first *in vivo* evidence that membrane localization of C3G can trigger activation of RAP1 and RAS resulting in the activation of MAPK, one of the hallmarks of v-*crk* transformation previously thought to be mediated through activation of SOS.

Keywords: C3G/CRK/*Drosophila*/RAP1/RAS–MAPK signaling

Introduction

Gaining insights into the molecular mechanisms underlying oncogenesis requires the identification of the cellular signal transduction pathways that are aberrantly activated during oncogenic transformation.

v-*crk* was isolated originally as an oncogene of a chicken retrovirus that transforms chicken embryonic fibroblasts and NIH 3T3 cells (Mayer *et al*., 1988; Greulich and Hanafusa, 1996). v-*crk* transformation leads to an elevation of tyrosine phosphorylation on characteristic proteins including the focal adhesion molecules p130^{cas} and PAXILLIN, and an increase in the activity of JUN kinase (JNK) and MAPK (Sakai *et al*., 1994; Clark and Brugge, 1995; Greulich and Hanafusa, 1996; Tanaka *et al*., 1997). The v-*crk* oncogene is unusual in that it encodes an adaptor protein, which is comprised of viral Gag sequences fused to the SH2 and the N-terminal SH3 domain of c-CRK (Mayer *et al*., 1988; Matsuda *et al*., 1992). Consistent with its identification as an adaptor protein, v-CRK has been shown to bind a number of cellular proteins via its SH2 domain, including the adaptor molecules c-CBL, p130^{cas} and PAXILLIN (reviewed in Birge *et al*., 1996). In addition, the v-CRK SH3 domain is capable of binding the tyrosine kinases ABL and ARG, the RAS guanine nucleotide exchange factor (GEF) SOS and the putative RAP1 GEF C3G (reviewed in Birge *et al*., 1996).

Due to the identification of these v-CRK-binding partners, progress has been made in the elucidation of the signal transduction mechanisms utilized in v-*crk* transformation. The ability of v-CRK to bind to the RAS family GEF SOS suggested an involvement of the RAS pathway. Expression of dominant-negative H-RAS^{N17} causes morphological reversion of v-*crk*-transformed NIH 3T3 cells, suggesting that RAS activation is involved in v-*crk* transformation (Greulich and Hanafusa, 1996). Since v-CRK binds much more strongly to C3G than to SOS (Knudsen *et al*., 1995), the C3G exchange factor is very likely to play a prominent role in v-*crk* transformation. This view is supported by the finding that expression of dominant-negative C3G can also cause morphological reversion of v-*crk*-transformed NIH 3T3 cells (Tanaka *et al*., 1997).

C3G was isolated originally as a binding partner for the SH3 domain of v-CRK (Knudsen *et al*., 1994; Tanaka *et al*., 1994). It contains a CDC25-homologous region, suggesting that C3G is a GEF for RAS GTPases. Biochemical studies have shown that, *in vitro*, C3G stimulates guanine nucleotide exchange on two RAS family members, RAP1 and R-RAS (Gotoh *et al*., 1995, 1997). However, the role of C3G in cellular signal transduction is still unclear, as is the role of RAP1 and R-RAS. On the one hand, C3G has been implicated in JNK activation, but the signal transduction mechanism by which this activation is achieved is not understood (Tanaka *et al*., 1997). In 293T cells, C3G-mediated activation of JNK could not be suppressed by co-expression of dominant-negative versions of RAP1, R-RAS or H-RAS, suggesting that C3G might act through an unknown RAS GTPase (Tanaka and Hanafusa, 1998). On the other hand, a recent study shows that C3G is involved in MAPK activation. During nerve growth factor (NGF)-induced differentiation of PC12 cells, MAPK initially is activated by RAS, but its activation is sustained by RAP1. C3G and CRK together activate RAP1, which then forms a stable complex with B-RAF, an activator of MAPK (Vossler *et al*., 1997; York *et al*., 1998).

To understand better the cellular signal transduction mechanisms utilized during v-*crk* transformation, we decided to clone and characterize C3G in *Drosophila* and to study its function in a developing organism. The signal transduction pathways involved in MAPK and JNK activation have been found to be highly conserved between flies and vertebrates (reviewed in Marshall, 1994, 1995; Minden and Karin, 1997; Ip and Davis, 1998; Noselli,

1998; Wassarman and Therrien, 1998), and the biological role of these pathways during development has been studied using an arsenal of tools, including dominant-active, dominant-negative and loss-of-function mutations. Activation of MAPK in *Drosophila* is thought to be triggered largely by receptor tyrosine kinase (RTK) signaling and to be mediated through RAS1, the *Drosophila* homolog of mammalian N-RAS, H-RAS and K-RAS, and then through the protein kinases KSR, RAF, MEK and MAPK. This RAS1–MAPK cassette is involved in both differentiation and proliferation of cells during *Drosophila* development (Lu *et al*., 1993; Karim and Rubin, 1998; Wassarman and Therrien, 1998). In contrast, the *Drosophila* JNK pathway, consisting of *Drosophila* JNKK/JNK/JUN and equivalent to the mammalian stress-activated MAPK pathway, appears to be involved predominantly in cell movement during morphogenesis (reviewed in Ip and Davis, 1998; Noselli, 1998).

Here we show that *Drosophila* C3G (DC3G) shares several regions of sequence homology with its human cognate, including the CDC25 catalytic domain and proline-rich motifs, which bind to CRK with high specificity. We find that during *Drosophila* eye and wing development, overexpression of membrane-tagged full-length DC3G phenotypically mimicks overactivation of the RAS1–MAPK pathway, suggesting that DC3G is involved in MAPK activation *in vivo*. Since these effects can be suppressed by a 50% reduction in the gene dose of RAS1–MAPK pathway components or RAP1, membrane-tagged DC3G is likely to stimulate both RAS1 and RAP1 directly, which in turn leads to a convergent activation of the MAPK pathway. Overexpression of a membrane-tagged version of DC3G lacking the CDC25 catalytic domain mimicks reduction in RAS1–MAPK signaling, but also leads to morphogenetic defects, whose causes remain to be elucidated.

Results

Identification of Drosophila C3G

To identify a *Drosophila* C3G homolog, we screened a *Drosophila* genomic library using hybridization with a human C3G (hC3G) cDNA probe containing only the CDC25-homologous region (Tanaka *et al*., 1994). Two true genomic clones were isolated and their CDC25-homologous region was used to screen a *Drosophila* cDNA library prepared from eye-imaginal discs under high stringency hybridization conditions (see Materials and methods). Over 30 cDNA clones were isolated and characterized. Restriction mapping indicated that they were all derived from the same locus, which we have named *DC3G*. *DC3G* is located in the 6C7–D2 interval on the *Drosophila* cytogenetic map.

The longest cDNA clones were only 3.1 kb in size, and clearly represent truncated cDNAs, as they detect a single mRNA of 7.0 kb on Northern blots of RNA prepared from imaginal discs (data not shown). Sequence analysis revealed that the cDNAs are truncated at the 5′ end, and 5′ RACE was carried out to recover the missing 5′ portion of the transcript, which is 4.0 kb in length, overlapping 0.3 kb with the longest cDNA clone. Sequence analysis of the composite revealed a single long open reading frame (ORF) encoding a protein of 1383 amino acids, with a predicted mol. wt of 151 kDa (Figure 1B). Comparison of DC3G with hC3G (Tanaka *et al*., 1994) identifies several domains with significant sequence similarity (Figure 1B and C). The very C-terminal region of the molecule (amino acids 1147–1383) contains the CDC25 catalytic domain, which is highly conserved between fly and human C3G (67% identity). There are two additional regions with significant sequence similarity (34% identity): a stretch of 116 amino acids in the N-terminal portion of the molecule (HD1) and a stretch of 236 amino acids immediately preceding the CDC25-homologous catalytic domain (HD2). The HD1 peptide is not found in any other protein in the database, and the significance of this motif is unclear. However, the HD2 peptide is conserved among GEFs acting on RAS proteins and may be involved in the recognition of the RAS GTPase (Lai *et al*., 1993).

In addition, DC3G contains eight putative SH3-binding motifs in the N-terminal portion of the molecule (Figure 1B and C), four of which fit the consensus sequence for binding by the N-terminal CRK SH3 domain (xPxLPxKxx; Knudsen *et al*., 1995). We tested binding of DC3G to CRK in a yeast two-hybrid assay (see Materials and methods). The region of DC3G which contains all of the putative SH3-binding motifs (amino acids 385–848) was fused to the GAL4 DNA-binding domain (‘bait’), while the SH3 domain of CRKs was fused to the GAL4 activation domain (‘prey’). Co-expression of these two constructs leads to high levels of expression of the *lacZ* reporter gene driven by the *UAS* promoter, suggesting a strong physical interaction between DC3G and the CRK SH3 domain (Figure 1D). Recently, the sequence of *Drosophila crk* (*DCrk*) has become available through the Berkeley Genome Project (Miklos and Rubin, 1996; Marra *et al*., 1998), and we have been able to show that the N-terminal SH3 domain of DCRK is also capable of interacting with DC3G in the yeast two-hybrid assay (data not shown). In contrast, the SH3 domains of DRK (Simon *et al*., 1993), the adaptor molecule involved in mediating the interaction between SOS and various RTKs (Olivier *et al*., 1993; Simon *et al*., 1993), do not show any interaction with DC3G in our assay (Figure 1D). These results indicate that the highly specific interaction between C3G and CRK is preserved between flies and vertebrates, suggesting a strong evolutionary conservation of CRK-mediated signaling.

Functional characterization of DC3G

DC3G maps to the 6C7–D2 interval on the cytogenetic map, a region for which neither point mutations nor deficiencies were available. In order to gain insight into the function of DC3G *in vivo*, we therefore decided to take a transgenic approach and to express activating and dominant-negative versions of the molecule in different tissues using the *UAS/GAL4* system (Brand and Perrimon, 1993). DC3G is expressed at a moderate level in all tissues throughout development, onto which higher levels of expression are superimposed in a tissue-specific manner (Figure 2). Overexpression of wild-type DC3G did not result in phenotypic abnormalities in the eye (data not shown). Since membrane targeting of SOS has been shown to be sufficient for activating the RAS signaling pathway in mammalian cells (Aronheim *et al*., 1994; Quilliam *et al*., 1994), we generated membrane-targeted versions of

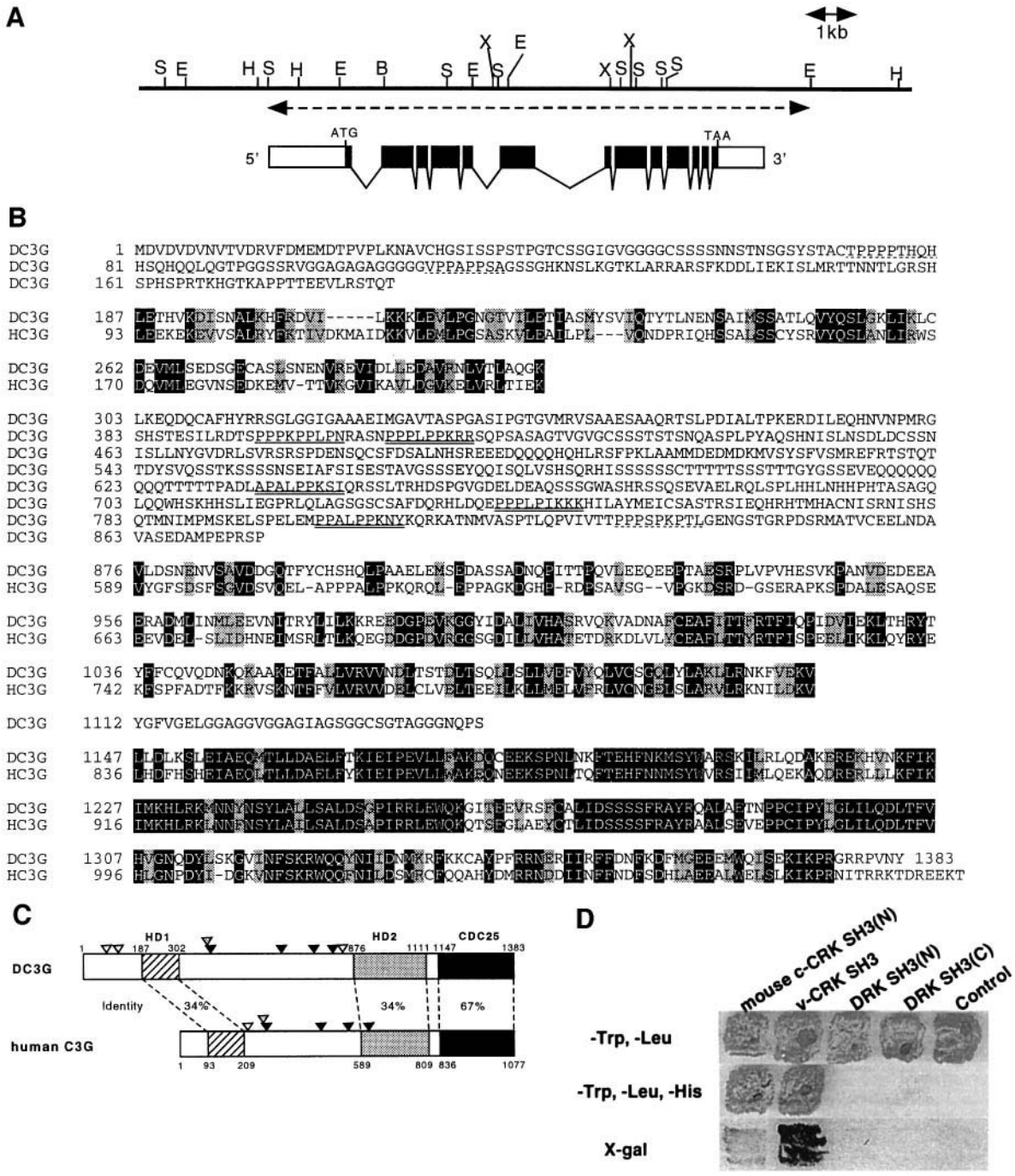

Fig. 1. Molecular characterization of DC3G. (**A**) A map of the genomic region encompassing *DC3G* showing *Bam*HI (B), *Eco*RI (E), *Hin*dIII (H), *Sal*I (S) and *Xho*I (X) restriction sites, and the structure of the *DC3G* transcript. The exon and intron structure was deduced from a comparison of 15 kb of genomic sequence (stippled arrow) with the sequence of the chimeric cDNA constructed from 5′ RACE and a cDNA clone isolated from an eye imaginal disc cDNA library (see Materials and methods); 5′ and 3′ UTRs are indicated by open bars, the ORF is indicated by a black bar. (**B**) The predicted amino acid sequence of the DC3G protein. A conceptual translation of the long ORF of the *DC3G* RNA transcript is shown. The translation begins at the first in-frame methionine codon, which is 1486 bases from the 5′ end of the transcript. The predicted DC3G protein sequence is compared with the sequence of hC3G. Residues are boxed wherever they are identical or similar to the DC3G protein sequence. Identical residues are boxed in black. Similar residues are boxed in gray. The following amino acids were considered similar: E, D; V, L, I, M; A, G; F, Y, W; S, T; Q, N; K, R. Putative SH3-binding motifs are underlined; unknown binding partner (dotted), $p130^{cas}$ (single; S.Ishimaru and K.Kirsch, unpublished observation), CRK (double). The DNA sequence of *DC3G* has been deposited in DDBJ/EMBL/GenBank joint databases under accession No. AF053358. (**C**) Schematic representation of the comparison between *Drosophila* and human C3G, showing the three major regions of sequence similarity and the distribution of SH3-binding motifs. Putative CRK N-terminal SH3-binding motifs are shown as black triangles, putative $p130^{cas}$ SH3-binding motifs are shown as gray triangles, putative SH3-binding motifs with unknown partner are shown as white triangles. (**D**) Yeast two-hybrid assay. Co-expression of DC3G fused to the GAL4 DNA-binding domain with SH3 domains of CRK and DRK fused to the GAL4 activation domain. Only the SH3 domains of v-CRK and the N-terminal SH3 domain of mouse c-CRK show a significant interaction, based on expression of *His3* and *lacZ* reporter genes.

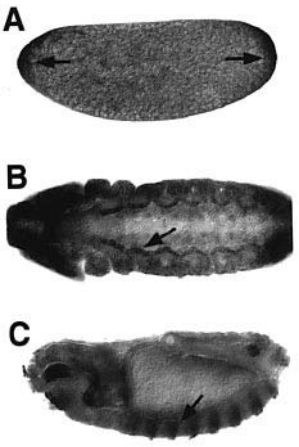

Fig. 2. *DC3G* transcript distribution during embryonic development. *In situ* hybridizations of embryos with a *DC3G* antisense RNA probe photographed under Nomarski optics; anterior to the left. (**A**) Sagittal view of a stage 4 embryo; high levels of *DC3G* transcript are found at the anterior and posterior poles (arrows), while lower levels of transcript are found throughout the embryo. (**B**) Ventral view of a stage 11 embryo; levels of *DC3G* transcript vary in a tissue-specific pattern. Note the particularly high levels of expression in the visceral mesoderm (arrow). (**C**) Lateral view of a late stage 14 embryo; *DC3G* transcript levels are increased in a segmentally repeated pattern (arrow), as well as in the fore- and hindgut. The pattern of high level DC3G expression resembles in part that of MAPK activation (Gabay *et al*., 1997).

DC3G (*UASMyDC3G*) to achieve overactivity ('activated DC3G'). In order to create a version of the molecule that would interfere with intrinsic DC3G activity, we truncated the membrane-tagged molecule so that it would lack the C-terminal CDC25 domain (*UASMyDC3G*Δ; 'dominant-negative DC3G'). The same truncation causes hC3G to act in a dominant-negative fashion, abolishing both the colony-forming potential and the increase in JNK activity of v-*crk* in NIH 3T3 cells (Tanaka *et al*., 1997). All constructs were engineered to contain a C-terminal MYC tag in order to facilitate assessment of transgene expression (Roth *et al*., 1991).

DC3G transgene expression in the developing eye

To explore the role of DC3G in cellular signaling, we examined the effects of *DC3G* transgenes in the developing adult eye. Owing to the fact that the eye lends itself particularly well to assaying dominant genetic interactions, the role of the RAS1–MAPK pathway in particular has been studied there in detail, largely in the context of R7 cell fate determination (reviewed in Wassarman and Therrien, 1997). Neuronal determination of the R7 precursor, as well as that of the other photoreceptor precursors, requires the activation of RAS1 and of the MAPK cascade. In the R7 precursor, this activation is triggered by activation of the SEVENLESS RTK, while it is thought to be triggered by epidermal growth factor receptor (EGFR) activation in the other R precursors (Freeman, 1996). Ectopic activation of components of the RTK–RAS1–MAPK pathway in the third instar larval eye disc leads to excessive neuronal determination (Basler *et al*., 1991; Dickson *et al*., 1992a,b; Fortini *et al*., 1992; Brunner *et al*., 1994), while attenuation of RAS1 signaling prevents neuronal determination of precursor cells (Therrien *et al*., 1995; Allard *et al*., 1996; Karim *et al*., 1996).

Expression of activated DC3G under *GMRGAL4* control, which drives expression in all cells posterior to the morphogenetic furrow in the developing eye (Ellis *et al*., 1993; Hay *et al*., 1995), leads to an adult rough eye phenotype with varying degrees of severity depending on the genomic insertion site of the transgene. Transgenic lines with intermediate phenotypes show a moderately rough eye surface with differentiated lenses and bristles (Figure 3B). Histological sections reveal that all ommatidia contain supernumerary photoreceptor cells, in some cases up to five or six additional cells (Figure 3F). Most of these supernumerary photoreceptor cells have small rhabdomeres and are located in the distal portion of the retina, suggesting that they are R7 cells. Some pigment cells are present, but fail to form a lattice surrounding the ommatidia. In transgenic lines with strong phenotypes, the adult eyes are reduced in size and their surface appears rough and folded (Figure 3C). There are very few bristles on the surface and lens facets are not discernible. Histological sections reveal a dramatic disruption of ommatidial architecture. Fewer clusters of photoreceptor cells are discernible, the number of cells per cluster and the arrangement of cells is irregular, and their rhabdomeres often do not span the entire thickness of the retina and show an elongated morphology (Figure 3G).

In order to establish that this apparent loss of photoreceptors in adults with strong phenotypes is not caused by early defects in neuronal cell fate determination, but occurs later as a consequence of abnormal morphogenesis, we examined developing eye discs of transgenic lines during the third instar larval stage using a pan-neural marker. ELAV, a neuron-specific RNA-binding protein, is expressed in all photoreceptor precursors as soon as they begin their terminal differentiation as neurons (Robinow and White, 1991). In discs with high levels of activated DC3G, the number of ELAV-positive cells is markedly increased. Additional cells sitting in between developing ommatidial clusters are visible, with the number of supernumerary cells increasing with the age of a row (Figure 3I and J). This result indicates that in eye discs with high levels of activated DC3G, early neural determination does occur and in fact occurs in excess, suggesting that the defects seen in adults are due to impairment of subsequent differentiation or morphogenesis. The phenotypic defects caused by activated DC3G are qualitatively similar to those caused by overactivity of the RAS1 pathway. Expression of $RAS1^{V12}$ under *GMRGAL4* control similarly leads to excessive neural determination of precursor cells in the eye disc (Figure 3K); however, the number of supernumerary neurons is larger than that generated by activated DC3G.

These phenotypic similarities suggest that activated DC3G activates the RAS1–MAPK pathway, either directly by serving as an exchange factor for RAS1, or indirectly, by serving as an exchange factor for another GTPase, whose activation then leads to the activation of the MAPK pathway. In order to determine whether, conversely, activated DC3G requires the function of the RAS1–MAPK pathway, we reduced the gene dose of *Ras1*, *ksr* and *rolled* (*rl*; MAPK) in the *GMRGAL4/UASMyDC3G* background by introducing one copy of complete loss-of-function alleles of these genes (see Materials and methods). We found that *Ras1*, *ksr* and *rl* all dramatically suppress the phenotype of activated DC3G (Figure 4B and G, C and

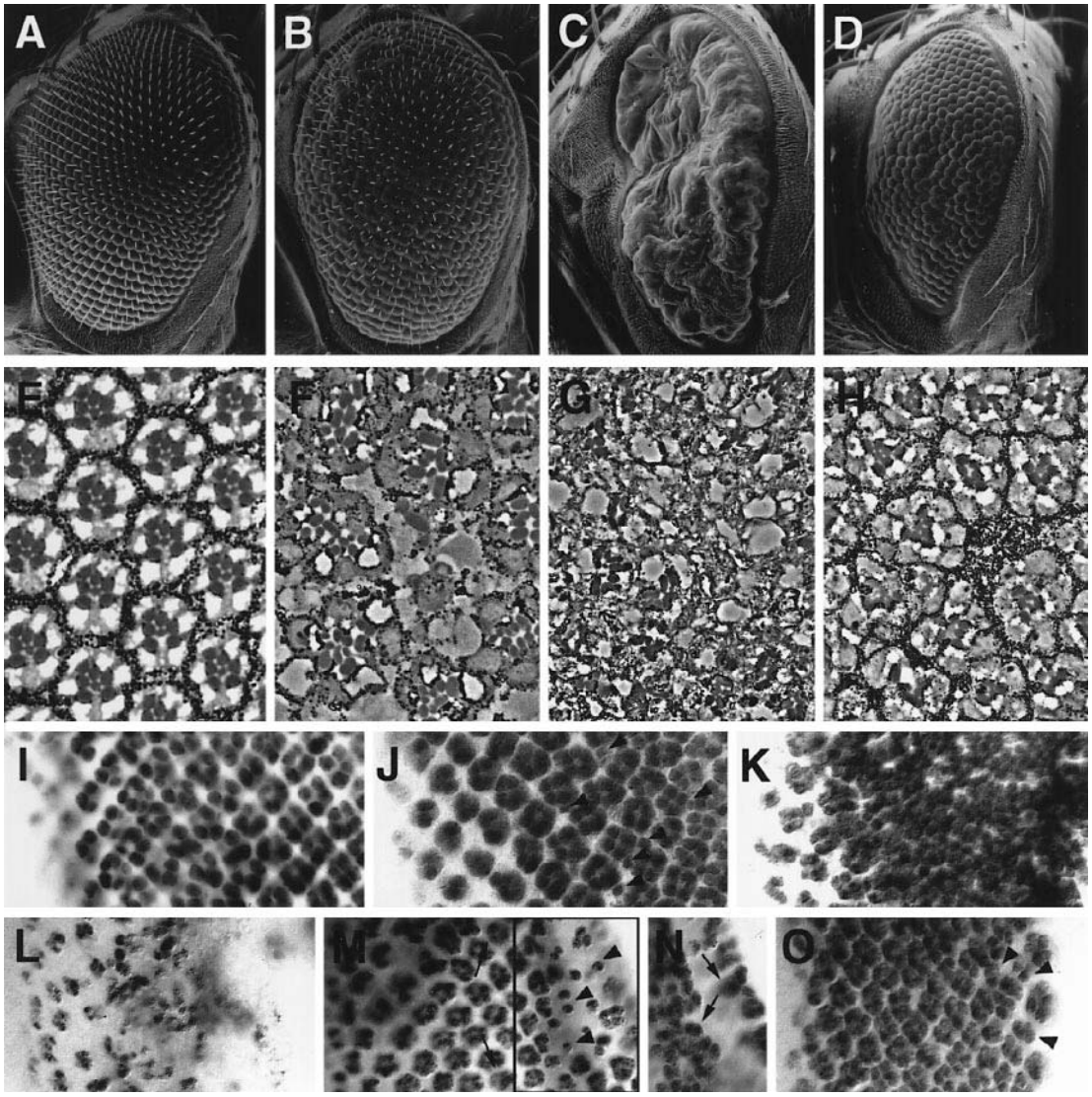

Fig. 3. Effects of *DC3G* transgene expression on eye development. (A–D) Scanning electron micrographs of adult eyes; anterior to the left, dorsal up. (E–H) Histological sections of adult eyes photographed under phase contrast. (I–O) Anti-ELAV stainings of third instar eye imaginal discs; posterior to the right. (**A**) and (**E**) Wild-type, (**B**) and (**F**) *GMRGAL4/UASMyDC3G* flies with intermediate phenotype. The external eye surface is moderately rough (B); sections show an increase in the number of photoreceptors, mostly R7 cells (F). (**C**) and (**G**) *GMRGAL4/UASMyDC3G* flies with strong phenotype. The eye appears collapsed, the surface folded with no discernible lenses and few bristles (C); sections reveal major disruption of ommatidial lattice (G). (**D**) and (**H**) *GMRGAL4/2×MyDC3GΔ* flies. (D) The eye is much narrower than in wild-type (A), and bristles are completely missing; (H) moderate loss of photoreceptors and irregularities in the pigment cell lattice. Note the randomized orientation of ommatidia with wild-type configuration. (**I**) Wild type, (**J**) *GMRGAL4/UASMyDC3G*, (**K**) *GMRGAL4/UASRas1V*^{12}, (**L**) *2×GMRGAL4/4×UASMyDC3GΔ*, (**M**) and (**N**) *GMRGAL4/3×UASMyDC3GΔ*, and (**O**) *GMRGAL4/UASRas1N*^{17} eye discs. Compared with wild-type (I), activated DC3G (J) and activated RAS1 (K) expression results in an increased number of ELAV-positive cells (J; arrowheads). The effect is more severe with activated RAS1. Conversely, expression of dominant-negative DC3G (L–N) and of dominant-negative RAS1 (O) led to a loss of ELAV-positive cells (arrowheads) in the posterior-most portion of the eye disc. In the *GMRGAL4/3×UASMyDC3GΔ* background, ELAV-positive nuclei are displaced basally; (N) is a basal optical section of boxed area in (M).

H, and D and I), while a reduction in the dose of *Sos* and *drk* had no effect on the phenotype (data not shown). Since biochemical studies have shown that hC3G serves as an exchange factor for RAP1 (Gotoh *et al*., 1995), we wanted to examine whether the function of *Drosophila* RAP1 is required for the expression of the activated DC3G phenotype. Reduction in *Rap1* gene dose by introducing one copy of a complete loss-of-function allele (see Materials and methods) also leads to a strong suppression of the activated DC3G phenotype (Figure 4E and J). Thus, not only does overactivation of DC3G lead to phenotypic defects similar to those evoked by activation of RAS1, but these defects are also suppressed efficiently by reducing the dose of genes in the RAS1–MAPK pathway, as well as by reducing the dose of *Rap1*. These findings indicate that the effects of DC3G overactivation are at least in part mediated by the RAS1–MAPK pathway and by RAP1.

Overexpression of dominant-negative DC3G under *GMRGAL4* control also severely affects eye development, but only when two or more copies of the *UAS* transgene are present. The adult eye is much reduced in size and often tear-shaped, indicating that development of the ventral part of the eye is more strongly affected than the dorsal part (Figure 3D). Lens facets are still formed, but bristles are completely absent. Histological sections reveal a reasonably well-formed pigment cell lattice surrounding

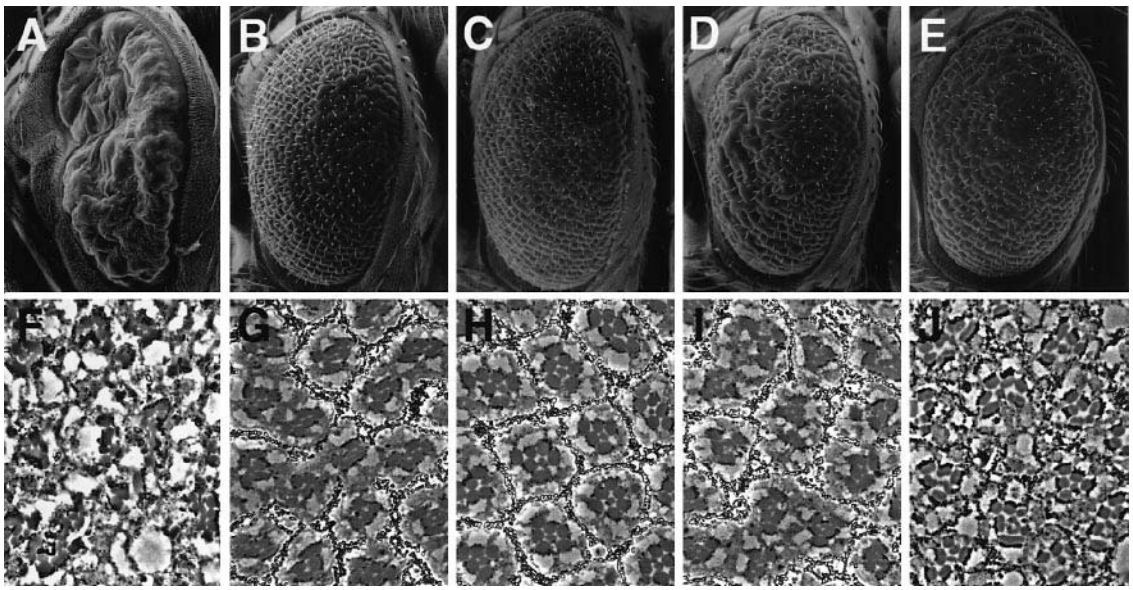

Fig. 4. Genetic interactions between activated DC3G and components of the RAS1–MAPK pathway and RAP1. (A–E) Scanning electron micrographs and (F–J) histological sections of adult eyes photographed under phase contrast. Dominant genetic interactions between the *GMRGAL4/UASMyDC3G* background shown in (**A** and **F**), and $Ras1^{e1B}$ (**B** and **G**), ksr^{S638} (**C** and **H**), rl^{x-3-30} (**D** and **I**) and $Rap1^{B1}$ (**E** and **J**). The drastic eye phenotype caused by strong expression of activated DC3G is greatly suppressed by a 50% reduction of the gene dose of RAS1–MAPK pathway components and of RAP1. The suppression by *ksr* and *Rap1* (H and J) is stronger than that by *Ras1* and *rl*.

the ommatidia, but the number of photoreceptors per ommatidium is often reduced by one or two cells (Figure 3H). Furthermore, as judged by ommatidia containing the normal complement of photoreceptors, the orientation of ommatidia is no longer parallel, but randomized instead (compare Figure 3H with E).

To determine whether dominant-negative DC3G interferes with RAS1–MAPK signaling, we compared the phenotypic defects resulting from expression of dominant-negative DC3G with those of dominant-negative $RAS1^{N17}$. Since expression of $RAS1^{N17}$ under *GMRGAL4* control results in the complete loss of the eye in the adult, the analysis was carried out at the third instar larval stage using ELAV as a marker for neuronal differentiation. Animals carrying three copies of dominant-negative C3G under *GMRGAL4* control show a marked decrease in the number of ELAV-positive cells posterior of the morphogenetic furrow, with the loss of cells becoming more severe with the age of a row (Figure 3M and N). In animals carrying four copies of dominant-negative C3G and two copies of GMRGAL4, ELAV staining is almost completely lost in the posterior-most portion of the eye disc (Figure 3L). Similarly, animals carrying one copy of $RAS1^{N17}$ under *GMRGAL4* control show a loss of ELAV-positive cells in the posterior-most portion of the eye disc (Figure 3O). Altogether, these findings strongly support the idea that dominant-negative DC3G interferes with RAS1–MAPK signaling in the developing eye. In further support of this interpretation, the effects of dominant-negative C3G are overridden by the concomitant expression of activated RAS1 (data not shown).

DC3G transgene expression in the developing wing

Apart from its role in differentiation, the RAS1–MAPK pathway has also been implicated in cell proliferation during *Drosophila* development. Expression of activated RAS1 ($RAS1^{V12}$) during imaginal disc development is sufficient to drive cell proliferation and hyperplastic tissue growth. This $RAS1^{V12}$-induced cell proliferation is dominantly suppressed by loss-of-function mutations in the genes encoding D-RAF, MAPK and KSR, suggesting that the MAPK pathway is involved in mediating the proliferative response (Karim and Rubin, 1998).

To determine whether DC3G can influence cell proliferation, we expressed the wild-type, activated and dominant-negative versions under the control of the decapentaplegic (*dpp*) disc enhancer fragment (*dppGAL4*; Staehling-Hampton *et al*., 1994). This enhancer fragment drives gene expression in all imaginal discs in a spatially restricted pattern closely resembling that of endogenous *dpp*. In the wing imaginal disc, *dppGAL4* is expressed in a broad stripe just anterior of the antero-posterior compartment border, which will run between the third and fourth vein in the adult wing. The expression patterns of the *DC3G* transgenes were visualized directly using anti-MYC antibodies.

Expression of wild-type DC3G under *dppGAL4* control (Figure 5A) results in a pattern indistinguishable from that of β-galactosidase under *dppGAL4* control (data not shown), showing that overexpression of wild-type DC3G does not affect cell proliferation. In contrast, expression of activated DC3G under *dppGAL4* control results in a gross distortion of the pattern (Figure 5B). Instead of forming a well-defined stripe, the staining is diffuse and broadened considerably, often to encompass large portions of the wing pouch. To determine whether activated DC3G induces cell proliferation, third instar larval discs were labeled with bromodeoxyuridine (BrdU), which is incorporated by cells during S phase. *dppGAL4/UAS-MyDC3G* wing discs show an increase in BrdU incorporation in a band corresponding to the domain of *dppGAL4* expression (data not shown). These findings indicate that

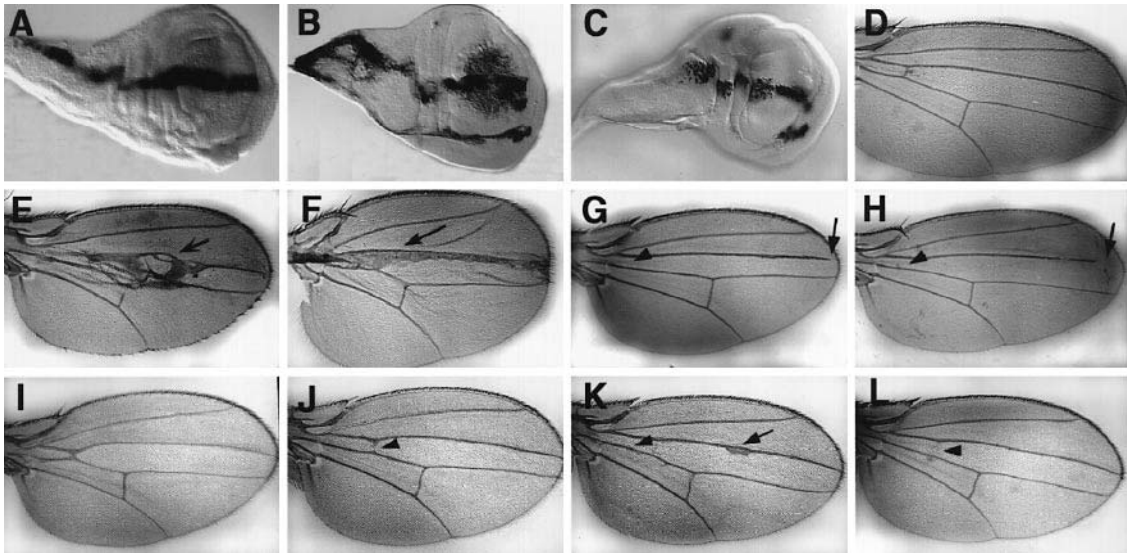

Fig. 5. Effects of DC3G transgene expression on wing development. (A–C) Third instar larval wing discs stained with anti-MYC antibodies, photographed with Nomarski optics, and (D–L) adult wings. (**A**) *dppGAL4/UASDC3G*, (**B**) *dppGAL4/UASMyDC3G* and (**C**) *dppGAL4/2×UASMyDC3GΔ*. Compared with expression of wild-type DC3G (A), the width of the stripe of cells expressing *dppGAL4*, and therefore the *myc*-tagged *DC3G* transgenes, is substantially increased when activated DC3G is expressed (B), and decreased when dominant-negative DC3G is expressed (C). (**D**) Wild-type, (**E**) *dppGAL4/UASMyDC3G* and (**F**) *dppGAL4/UASRas1^{V12}*; the third vein (arrows) is broadened. (**G**) *dppGAL4/2×UASMyDC3GΔ* and (**H**) *dppGAL4/UASRas1^{N17}*; the anterior cross vein is missing (arrowhead), the third vein does not reach the wing margin (arrow) and is disrupted when dominant-negative RAS1 is expressed (H). (I–L) Dominant genetic interactions between the *dppGAL4/UASMyDC3G* background shown in (E), and *Ras1^{e1B}* (**I**), *ksr^{S638}* (**J**), *rl^{x-3-30}* (**K**) and *Df(3L)R^{G7}*(**L**). The broadening of the third wing vein is completely suppressed by a 50% reduction of the gene dose of *Ras1*, *ksr* and *Rap1*, and only partially by *rl* (arrow, K). In all cases, the anterior cross vein is affected or missing (arrowheads), which is also observed with dominant-negative DC3G (G) and dominant-negative RAS1 (H).

activated DC3G drives the cells in which it is expressed to overproliferate.

Adult wings of *dppGAL4/UASMyDC3G* flies display a massive broadening of the third vein (Figure 5E). Similarly, expression of RAS1^{V12} under *dppGAL4* control results in overproliferation of cells in the wing disc which express the transgenes (Karim and Rubin, 1998), and subsequently also to a vast broadening of the third vein in the adult wing (Figure 4F; Karim and Rubin, 1998). The adult wing phenotype of *dppGAL4/UASMyDC3G* flies is completely suppressed by reducing the gene dose of *Ras1*, *Ksr*, *rl* and *Rap1* (Figure 5I–L), while a reduction in the dose of *Sos* and *drk* has no effect on the phenotype (data not shown), indicating that activated DC3G also requires the function of the RAS1–MAPK pathway and of RAP1 in the wing.

Conversely, expression of dominant-negative C3G under *dppGAL4* control leads to a narrowing of the stripe of expression in the disc (Figure 5C). In the adult, the third vein fails to reach the wing margin and the anterior cross vein is missing (Figure 5G), which again resembles the phenotype of dominant-negative RAS1^{N17} under *dppGAL4* control (Figure 5H).

Discussion

The strong conservation of signal transduction pathways between vertebrates and *Drosophila* encouraged us to use the fly as a model to study the mechanisms underlying v-*crk* transformation. As a first step, we isolated the *Drosophila* homolog of C3G, a RAS family GEF, which had first been identified in humans on the basis of its strong physical interaction with the SH3 domain of v-CRK (Knudsen *et al*., 1994; Tanaka *et al*., 1994). Both the strength of this interaction and the ability of dominant-negative C3G to interfere with v-*crk* transformation (Tanaka *et al*., 1997) argue that C3G plays an essential role in this transformation.

Sequence comparison between *Drosophila* and human C3G strongly suggests that DC3G is a true ortholog. Not only does the CDC25 catalytic domain show a high degree of sequence conservation (67%), but the two molecules also share two additional domains of extensive sequence similarity. Similar to hC3G, DC3G also binds the N-terminal SH3 domain of CRKs, but not those of DRK, the *Drosophila* ortholog of vertebrate GRB2, suggesting a strong evolutionary conservation of the specificity of the CRK–C3G interaction. Given our interest in understanding the mechanisms of v-*crk* transformation, our primary focus was to study the effects of C3G overactivity.

DC3G can activate the MAPK pathway

Several lines of evidence suggest that DC3G has a role in activating the MAPK pathway. (i) The phenotypic defects resulting from overactivation of DC3G resemble those of RAS1–MAPK overactivation. This is true for both of the situations examined. The actual phenotypic consequences of the overactivation depend on the specific context, with either cell fate determination or cell proliferation affected. (ii) The phenotypic defects resulting from DC3G overactivation are strongly suppressed by reducing the gene dose of components of the RAS1–MAPK pathway. A 50% reduction in gene activity of *Ras1*, *ksr* and *rl* (MAPK) leads to a remarkable phenotypic rescue, while reduction in the gene dose of *Sos* or *drk* has no effect on the phenotype. (iii) The phenotypic defects resulting from expression of dominant-negative DC3G mimic the defects resulting from interference with the RAS1–MAPK path-

way (see below). Taken together, these findings show that DC3G can activate the RAS1–MAPK pathway.

This activation could be achieved either by direct stimulation of RAS1 or, indirectly, by stimulating another RAS family GTPase, which in turn activates RAS1. Several independent biochemical studies have shown that hC3G acts as a GEF for RAS family members *in vitro* (Gotoh *et al*., 1995, 1997). It is most efficient against RAP1, less so toward R-RAS, and only weakly active against H-RAS. Nevertheless, the possibility that *in vivo* DC3G directly activates RAS1, the *Drosophila* H-RAS homolog, cannot be discounted. The transgenes provide high levels of membrane-tagged DC3G, such that its local concentration at the membrane may be high enough to drive guanine nucleotide exchange on the less favored RAS1 substrate. In *Saccharomyces cerevisiae*, the hC3G catalytic domain is capable of rescuing the lethality of CDC25 (Tanaka *et al*., 1994), which encodes an exchange factor for RAS (Jones *et al*., 1991), the yeast H-RAS homolog, suggesting that there is appreciable catalytic activity of the C3G CDC25 domain toward RAS *in vivo*.

Alternatively, DC3G may activate the RAS1–MAPK pathway indirectly by activating R-RAS or RAP1. However, during eye development, expression of activated R-RAS leads to a loss of photoreceptor cells (Fortini *et al*., 1992), the phenotype opposite to that of activated DC3G and activated RAS1. This excludes the possibility that R-RAS acts as the relevant intermediary between DC3G and RAS1.

The effects of activated RAP1 on eye development currently are unknown. The function of *Rap1* has been studied mostly using viable alleles, such as the *Roughened* mutation, which cause a loss of predominantly the R7 photoreceptor in the eye (Hariharan *et al*., 1991; Li *et al*., 1997). The genetic classification of these alleles is somewhat unclear, making it difficult to extrapolate what the phenotypic consequences of RAP1 overactivity might be. To resolve this, we generated a transgene containing wild-type *Rap1* under *UAS* promoter control (*UASRap1*) and expressed it in the developing eye using *GMRGAL4*. The phenotype of *Rap1* overexpression is very similar to activated DC3G and is characterized by morphogenetic defects and, most importantly, by the presence of supernumerary photoreceptor cells (S.Ishimaru and U.Gaul, unpublished observation). This finding, together with the fact that the activated DC3G phenotype is strongly suppressed by a 50% reduction in *Rap1* gene dose using complete loss-of-function alleles, strongly argues that RAP1 activation is involved in generating the DC3G overactivity phenotype.

The fact that both RAS1 and RAP1 loss-of-function mutations suppress the DC3G overactivity phenotype, and the fact that the RAP1 overactivity phenotype resembles that of RAS1 overactivity, imply that RAS1 and RAP1 act in concert. This could be achieved by DC3G's stimulation of RAP1, with RAP1 in turn triggering RAS1 activation. Alternatively, DC3G could stimulate both RAS1 and RAP1 directly, possibly leading to a convergent activation of the MAPK pathway.

Further genetic and biochemical experiments will be required to discriminate between the two possibilities, as the role of RAP1 proteins vis-á-vis RAS is generally not well understood and, at least in vertebrates, is likely to be cell type dependent. Although RAP1 proteins originally were found to act as antagonists of v-*Ki-Ras* in NIH 3T3 cell transformation (Kitayama *et al*., 1989), later studies implied concerted action between the two, as both RAS and RAP1 exhibited mitogenic effects in Swiss 3T3 cells (Yoshida *et al*., 1992). Recent reports have also suggested that RAS and RAP1 can act in concert. RAP1 has been shown to activate B-RAF and the MAPK pathway in a RAS-independent manner during cAMP-induced neuronal differentiation of PC12 cells (Vossler *et al*., 1997). Thus, in this case, RAP1 can activate MAPK signaling in response to stimuli distinct from RTK-RAS activation of MAPK. Similarly in the fly, RAP1 may activate the MAPK pathway by directly stimulating the *Drosophila* homolog of the RAF protein family, D-RAF.

Which upstream factor(s) are likely to trigger DC3G-mediated activation of RAP1 in the developing eye and wing? In both contexts, EGFR activity is thought to be the major trigger for activation of the MAPK pathway by recruiting the DRK–SOS complex to the membrane, thereby effecting stimulation of RAS1. Since the cytoplasmic domain of EGFR contains one putative DRK SH2-binding motif (YXNX; Songyang *et al*., 1994) at position 1356 (YYND; Clifford and Schüpbach, 1994), the activated receptor may be able to interact directly with DRK; however, docking proteins such as DOS or D-SHC may also play a role (Lai *et al*., 1995; Herbst *et al.*, 1996; Raabe *et al*., 1996). It seems possible that the recruitment of CRK-bound C3G to the plasma membrane, leading to RAP1 stimulation, is also triggered by EGFR activity. Since the cytoplasmic domain of EGFR contains two putative CRK SH2-binding sites (YXXP; Birge *et al*., 1992; Sakai *et al*., 1994) at positions 1198 (YLQP) and 1252 (YLMP) (Clifford and Schüpbach, 1994), the activated receptor may also interact directly with the CRK adaptor. Thus, CRK, C3G and RAP1 may provide an alternate route by which EGFR can stimulate the MAPK pathway.

The biological effects of dominant-negative DC3G

The biological effects of expression of dominant-negative DC3G, although not quite as robust as those achieved by activated DC3G, strongly suggest that dominant-negative DC3G is indeed interfering with signaling of the RAS1–MAPK cascade. In the wing, dominant-negative DC3G fully mimicks the effects of dominant-negative RAS1, namely underproliferation, which is the opposite phenotype of activated DC3G and RAS1. In the eye, the effect of dominant-negative DC3G appears to be more dose dependent. Increasing numbers of transgene copies lead to an ever greater reduction in eye size and an ever greater loss of photoreceptors, reflecting an increasing interference with the RAS1–MAPK pathway. The difference in dosage sensitivity between the two tissues may be due to differences in the activity levels of the MAPK pathway.

The mechanism of v-crk transformation and DC3G-mediated signal transduction

During v-*crk* transformation, CRK-binding proteins, including SOS and C3G, become localized to the plasma membrane and focal adhesion points at high concentrations (Nievers *et al*., 1997), leading to abnormal activation of the MAPK and JNK pathways and morphological

transformation (Birge *et al*., 1996). MAPK activation was thought to be mediated by v-CRK's interaction with SOS, whereas activation of JNK was thought to be mediated by its interaction with C3G (Teng *et al*., 1995; Birge *et al*., 1996; Tanaka *et al*., 1997). However, our *in vivo* analysis shows that membrane binding of DC3G leads to strong activation of MAPK signaling. Our finding of DC3G stimulating MAPK activity appeared to conflict with a previous study, which had reported that in 293T cells expression of wild-type C3G led to a mild activation of JNK, but not of MAPK (Tanaka *et al*., 1997). To address this discrepancy, we tested the ability of membrane-tagged DC3G to induce MAPK activation in 293T cells and found a 3-fold induction of MAPK activity (S.Ishimaru and T.Shishido, unpublished observation), arguing that MAPK activation can be triggered at higher local concentrations of C3G at the membrane. In addition, in a very recent report, York *et al*. (1998) demonstrate that CRK-bound C3G leads to RAP1 activation, which in turn leads to sustained activation of MAPK in PC12 cells, lending further support to our findings. Further studies are underway to elucidate the role of DC3G in JNK signaling.

Materials and methods

Molecular cloning and DNA sequencing

An EMBL3 *Drosophila* genomic library (Tamkun *et al*., 1992) was screened under low stringency conditions using the CDC25-homologous region of hC3G (residues 774–1077; Tanaka *et al*., 1994) as a probe; the hybridization was performed in 5× SSCP, 10× Denhardt's, 0.2% SDS and 25% formamide at 42°C and the final wash was carried out in 0.5× SSC containing 0.5% SDS at 42°C. Of the 12 clones obtained by the inital screening (9625-1 to 9625-12), two true positive clones (9625-9 and -12) were selected by PCR using degenerate oligonucleotide primers corresponding to amino acid sequences QLT(I/V/L)L(D/E) and (V/I)NFSK(R/M), respectively, which are conserved amino acids sequences among CDC25-homologous domains. With the above PCR fragment (corresponding to residues 1158–1323 of DC3G protein) as a probe, we screened an eye imaginal disc cDNA library in λgt10 (constructed by A.Cowman) using standard methods (Sambrook *et al*., 1989). 5′ RACE (Marathon amplification kit, Clontech) was carried out to amplify a cDNA fragment containing the 5′ end of the gene. The inital 5′ RACE was performed with the adaptor primer (AP) 1 (5′-CCATCCTAATACGACTCACTATAGGGC-3′) and the 6821-1′ primer (5′-GCCTTGCGCTGCTTGTAGTTCTTTGGC-3′; complementary to nucleotides 3641–3668 within the full-length cDNA sequence). AP2 (5′-ACTCACTATAGGGCTCGAGCGGC-3′) and 6816-1′(5′-TTCGATCA-GGCTGTGGTGCTT-3′; complementaty to nucleotides 3351–3371 in the full-length cDNA sequence) were used for nested PCR. The resulting 5′ RACE fragment contained nucleotides 1–3371 within the full-length cDNA sequence. cDNAs and the corresponding genomic regions were subcloned into pBluescriptII (Stratagene) for DNA sequencing. DNA was sequenced by the dideoxy chain termination method (Sanger *et al*., 1980) with vector-specific primers on Applied Biosystems 373A and 377 DNA sequencers (Rockefeller University Protein/DNA Technology Center).

Generation of DC3G transgenic strains

Amplificaion of 6× myc tags derived from pCS2+MT (Roth *et al*., 1991) was by PCR using specific primers to add appropriate restriction sites. The full-length *DC3G* clone was constructed by generating a chimera between an RT–PCR clone containing the 5′ region and DC3-34, the longest cDNA clone isolated from the eye imaginal disc cDNA library. The *DC3G*Δ construct was generated by deleting the 3′ region encoding the CDC25-homologous domain (corresponding to amino acid residues 1145–1383). The *DC3G* constructs were modified by PCR in order to allow in-frame fusion with the 6× myc tag. We also used PCR with appropriate primers to add the myristylation signal from c-SRC (MGSSKSKPKDPSQR; Resh, 1994) to the 5′ termini of *DC3G* constructs. All *DC3G* constructs were inserted into the pUAST vector (Brand and Perrimon, 1993) after modification and injected into w^{1118} embryos as previously described (Karess and Rubin, 1986).

Fly strains

GAL4 driver strains and additional *UAS* strains were generously provided by M.Freeman (*GMRGAL4*), U.Heberlein (*dppGAL*), C.Klämbt (*UAS-Ras1*^{V12}) and D.Montell (*UASRas1*^{N17}). *Ras1*^{e1B}, *Sos*^{e4G} and *drk*^{e0A} were a gift from M.Simon, *ksr*^{S638} and *rl*$^{x-3-30}$ from H.Chang, and *Rap1*^{B1} from I.Hariharan. All these mutations present complete loss-of-function alleles of their respective loci.

Histology and immunocytochemistry

Larval cuticles were prepared according to van der Meer (1977). Wings were dissected, dipped in 100% ethanol and mounted in DPX (Fluka). Samples for scanning electron microscopy were prepared as described by Kimmel *et al*. (1990). Fixation and sectioning of adult *Drosophila* eyes were performed as described by Tomlinson and Ready (1987).

Antibody stainings of imaginal discs were carried out as described in Gaul *et al*. (1992). Rat anti-ELAV antibodies (generous gift from G.M.Rubin) were used at 1:2000, mouse anti-MYC antibodies at 1:400 (9E10, Santa Cruz Biotechnology) and horseradish peroxidase-coupled secondary antibodies (Jackson) at 1:200.

Acknowledgements

We thank Drs H.Chang, M.Freeman, I.Hariharan, U.Heberlein, C.Klämbt, D.Montell, G.M.Rubin and M.Simon for providing reagents, and Sung-Yun Yu and Dr N.Baker for help with the scanning electron microscopy. We would also like to thank S.Dinardo and members of the Gaul and Hanafusa labs for useful discussions during this work and helpful comments on the manuscript. This work was supported by a Charles H.Revson/Norman and Roista Winston Foundation fellowship to S.I., a Sinsheimer Award to U.G. and NCI grant #44356 to H.H. S.I was also supported in part by The Mochida Memorial Foundation for Medical and Pharmaceutical Research. U.G. is a McKnight Scholar.

References

Allard,J.D., Chang,H.C., Herbst,R., McNeill,H. and Simon,M.A. (1996) The SH2-containing tyrosine phosphatase corkscrew is required during signaling by sevenless, Ras1 and Raf. *Development*, **122**, 1137–1146.

Aronheim,A., Engelberg,D., Li,N., al-Alawi,N., Schlessinger,J. and Karin,M. (1994) Membrane targeting of the nucleotide exchange factor Sos is sufficient for activating the Ras signaling pathway. *Cell*, **78**, 949–961.

Basler,K., Christen,B. and Hafen,E. (1991) Ligand-independent activation of the Sevenless receptor tyrosine kinase changes the fate of cells in the developing *Drosophila* eye. *Cell*, **64**, 1069–1081.

Birge,R., Fajardo,J., Mayer,B.J. and Hanafusa,H. (1992) Tyrosine phosphorylated epidermal growth factor receptor and cellular p130 provide high affinity binding substrates to analyse Crk-phosphotyrosine-dependent interactions *in vitro*. *J. Biol. Chem.*, **267**, 10588–10595.

Birge,R.B., Knudsen,B.S., Besser,D. and Hanafusa,H. (1996) SH2 and SH3-containing adaptor proteins: redundant or independent mediators of intracellular signal transduction. *Genes Cells*, **1**, 595–613.

Brand,A.H. and Perrimon,N. (1993) Targeted gene expression as a means of altering cell fates and generating dominant phenotypes. *Development*, **118**, 401–415.

Brunner,D., Oellers,N., Szabad,J., Biggs,W.H., Zipursky,S.L. and Hafen,E. (1994) A gain-of-function mutation in *Drosophila* MAP kinase activates multiple receptor tyrosine kinase signaling pathways. *Cell*, **76**, 875–888.

Clark,E.A. and Brugge,J.S. (1995) Integrins and signal transduction pathways: the road taken. *Science*, **268**, 233–239.

Clifford,R. and Schüpbach,T. (1994) Molecular analysis of the *Drosophila* EGF receptor homolog reveals that several genetically defined classes of alleles cluster in subdomains of the receptor protein. *Genetics*, **137**, 531–550.

Dickson,B., Sprenger,F. and Hafen,E. (1992a) Prepattern in the developing *Drosophila* eye revealed by an activated torso–sevenless chimeric receptor. *Genes Dev.*, **6**, 2327–2339.

Dickson,B., Sprenger,F., Morrison,D. and Hafen,E. (1992b) Raf functions downstream of Ras1 in the Sevenless signal transduction pathway. *Nature*, **360**, 600–603.

Ellis,M.C., O'Neill,E.M. and Rubin,G.M. (1993) Expression of *Drosophila* glass protein and evidence for negative regulation of its activity in non-neuronal cells by another DNA-binding protein. *Development*, **119**, 855–865.

Fortini,M.E., Simon,M.A. and Rubin,G.M. (1992) Signalling by the sevenless protein tyrosine kinase is mimicked by Ras1 activation. *Nature*, **355**, 559–561.

Freeman,M. (1996) Reiterative use of the EGF receptor triggers differentiation of all cell types in the *Drosophila* eye. *Cell*, **87**, 651–660.

Gabay,L., Seger,R. and Shilo,B.Z. (1997). MAP kinase *in situ* activation atlas during *Drosophila* embryogenesis. *Development*, **124**, 3535–3541.

Gaul,U., Mardon,G. and Rubin,G.M. (1992) A putative Ras GTPase activating protein acts as a negative regulator of signaling by the Sevenless receptor tyrosine kinase. *Cell*, **68**, 1007–1019.

Gotoh,T. *et al*. (1995) Identification of Rap1 as a target for the Crk SH3 domain-binding guanine nucleotide-releasing factor C3G. *Mol. Cell. Biol.*, **15**, 6746–6753.

Gotoh,T., Niino,Y., Tokuda,M., Hatase,O., Nakamura,S., Matsuda,M. and Hattori,S. (1997) Activation of R-Ras by Ras-guanine nucleotide-releasing factor. *J. Biol. Chem.*, **272**, 18602–18607.

Greulich,H. and Hanafusa,H. (1996) A role for Ras in v-Crk transformation. *Cell Growth Differ.*, **7**, 1443–1451.

Hariharan,I.K., Carthew,R.W. and Rubin,G.M. (1991) The *Drosophila roughened* mutation: activation of a rap homolog disrupts eye development and interferes with cell determination. *Cell*, **67**, 717–722.

Hay,B.A., Wassarman,D.A. and Rubin,G.M. (1995) *Drosophila* homologs of baculovirus inhibitor of apoptosis proteins function to block cell death. *Cell*, **83**, 1253–1262.

Herbst,R. Carroll,P.M., Allard,J.D., Schilling,J., Raabe,T. and Simon,M.A. (1996) Daughter of Sevenless is a substrate of the phosphotyrosine phosphatase Corkscrew and functions during Sevenless signaling. *Cell*, **85**, 899–909.

Ip,Y.T and Davis,R.J. (1998) Signal transduction by the c-Jun N-terminal kinase (JNK)—from inflammation to development. *Curr. Opin. Cell Biol.*, **10**, 205–219.

Jones,S., Vignais,M.L. and Broach,J.R. (1991) The CDC25 protein of *Saccharomyces cerevisiae* promotes exchange of guanine nucleotides bound to ras. *Mol. Cell. Biol.*, **11**, 2641–2646.

Karess,R.E. and Rubin,G.M. (1984) Analysis of P transposable element functions in *Drosophila. Cell*, **38**, 135–146.

Karim,F.D. and Rubin,G.M. (1998) Ectopic expression of activated Ras1 induces hyperplastic growth and increased cell death in *Drosophila* imaginal tissues. *Development*, **125**, 1–9.

Karim,F.D., Chang,H.C., Therrien,M., Wassarman,D.A., Laverty,T. and Rubin,G.M. (1996) A screen for genes that function downstream of Ras1 during *Drosophila* eye development. *Genetics*, **143**, 315–329.

Kimmel,B.E., Heberlein,U. and Rubin,G.M. (1990) The homeo domain protein rough is expressed in a subset of cells in the developing *Drosophila* eye where it can specify photoreceptor cell subtype. *Genes Dev.*, **4**, 712–727.

Kitayama,H., Sugimoto,Y., Matsuzaki,T., Ikawa,Y. and Noda,M. (1989) A *ras*-related gene with transformation suppressor activity. *Cell*, **56**, 77–84.

Knudsen,B.S., Feller,S.M. and Hanafusa,H. (1994) Four proline-rich sequences of the guanine-nucleotide exchange factor C3G bind with unique specificity to the first Src homology 3 domain of Crk. *J. Biol. Chem.*, **269**, 32781–32787.

Knudsen,B.S., Zheng,J., Feller,S.M., Mayer,J.P., Burrell,S.K., Cowburn,D. and Hanafusa,H. (1995) Affinity and specificity requirements for the first Src homology 3 domain of the Crk proteins. *EMBO J.*, **14**, 2191–2198.

Lai,C.C., Boguski,M., Broek,D. and Powers,S. (1993) Influence of guanine nucleotides on complex formation between Ras and CDC25 proteins. *Mol. Cell. Biol.*, **13**, 1345–1352.

Lai,K.-M.V., Olivier,J.P., Gish,G.D., Henkemeyer,M., McGlade,J. and Pawson,T. (1995) A *Drosophila shc* gene product is implicated in signaling by the DER receptor tyrosine kinase. *Mol. Cell. Biol.*, **15**, 4810–4818.

Li,Q., Hariharan,I.K., Chen,F., Huang,Y. and Fischer,J.A. (1997) Genetic interactions with *Rap1* and *Ras1* reveal a second function for the Fat facets deubiquitinating enzyme in *Drosophila* eye development. *Proc. Natl Acad. Sci. USA*, **94**, 12515–12520.

Lu,X., Chou,T.B., Williams,N.G., Roberts,T. and Perrimon,N. (1993) Control of cell fate determination by p21ras/Ras1, an essential component of *torso* signaling in *Drosophila. Genes Dev.*, **7**, 621–632.

Marra,M.A., Hillier,L. and Waterston,R.H. (1998) Expressed sequence tags—ESTablishing bridges between genomes. *Trends Genet.*, **14**, 4–7.

Marshall,C.J. (1994) MAPK kinase kinase kinase, MAPK kinase kinase and MAPK kinase. *Curr. Opin. Genet. Dev.*, **4**, 82–89.

Marshall,C.J. (1995) Specificity of receptor tyrosine kinase signaling: transient versus sustained extracellular signal-regulated kinase activation. *Cell*, **80**, 179–185.

Matsuda,M., Tanaka,S., Nagata,S., Kojima,A., Kurata,T. and Shibuya,M. (1992) Two species of human CRK cDNA encode proteins with distinct biological activities. *Mol. Cell. Biol.*, **12**, 3482–3489.

Mayer,B.J., Hamaguchi,M. and Hanafusa,H. (1988) A novel viral oncogene with structural similarity to phospholipase C. *Nature*, **332**, 272–275.

Miklos,G.L.G. and Rubin,G.M. (1996) The role of the genome project in determing gene function: insights from model organisms. *Cell*, **86**, 521–529.

Minden,A. and Karin,M. (1997) Regulation and function of the JNK subgroup of MAP kinases. *Biochim. Biophys. Acta*, **1333**, F85–F104.

Nievers,M., Birge,R., Greulich,H., Verkleij,A., Hanafusa,H. and Henegouwen,P. (1997) v-Crk-induced cell transformation: changes in focal adhesion composition and signaling. *J. Cell Sci.*, **110**, 389–399.

Noselli,S. (1998) JNK signaling and morphogenesis in *Drosophila. Trends Genet.*, **14**, 33–38.

Olivier,J.P., Raabe,T., Henkemeyer,M., Dickson,B., Mbamalu,G., Margolis,B., Schlessinger,J., Hafen,E. and Pawson,T. (1993) A *Drosophila* SH2–SH3 adaptor protein implicated in coupling the Sevenless tyrosine kinase to an activator of Ras guanine nucleotide exchange, Sos. *Cell*, **73**, 179–191.

Quilliam,L.A., Huff,S.Y., Rabun,K.M.,Wei,W., Park,W., Broek,D. and Der,C.J. (1994) Membrane-targeting potentiates guanine nucleotide exchange factor CDC25 and SOS1 activation of Ras transforming activity. *Proc. Natl Acad. Sci. USA*, **91**, 8512–8516.

Raabe,T., Riesgo-Escovar,J., Liu,X., Bausenwein,B.S., Deak,P., Maröy,P. and Hafen,E. (1996) DOS, a novel pleckstrin homology domain-containing protein required for signal transduction between Sevenless and Ras1 in *Drosophila. Cell*, **85**, 911–920.

Resh,M.D. (1994) Myristylation and palmitylation of Src family members: the fats of the matter. *Cell*, **76**, 411–413.

Robinow,S. and White,K. (1991) Characterization and spatial distribution of the ELAV protein during *Drosophila melanogaster* development. *J. Neurobiol.*, **22**, 443–461.

Roth,M.B., Zahler,A.M. and Stolk,J.A. (1991) A conserved family of nuclear phosphoproteins localized to sites of polymerase II transcription. *J. Cell Biol.*, **115**, 587–596.

Sakai,R., Iwamatsu,A., Hirano,N., Ogawa,S., Tanaka,T., Mano,H., Yazaki,Y. and Hirai,H. (1994) A novel signaling molecule, p130, forms stable complexes *in vivo* with v-Crk and v-Src in a tyrosine phosphorylation-dependent manner. *EMBO J.*, **13**, 3748–3756.

Sambrook,J., Fritsch,E.F. and Maniatis,T. (1989) *Molecular Cloning: A Laboratory Manual*. Cold Spring Harbor Laboratory Press, Cold Spring Harbor, NY.

Sanger,F., Nicklen,S. and Coulson,A.R. (1977) DNA sequencing with chain-terminating inhibitors. *Proc. Natl Acad. Sci. USA*, **74**, 5463–5467.

Simon,M.A., Dodson,G.S. and Rubin,G.M. (1993) An SH3–SH2–SH3 protein is required for p21Ras1 activation and binds to Sevenless and Sos proteins *in vitro. Cell*, **73**, 169–177.

Songyang,Z. *et al*. (1994) Specific motifs recognized by the SH2 domains of Csk, 3BP2, fps/fes, GRB2, SHC, Syk, and Vav. *Mol. Cell. Biol.*, **14**, 2777–2785.

Staehling-Hampton,K., Hoffmann,F.M., Baylies,M.K., Rushton,E. and Bate,M. (1994) *dpp* induces mesodermal gene expression in *Drosophila. Nature*, **372**, 783–786.

Tamkun,J.W., Deuring,R., Scott,M.P., Kissinger,M., Pattatucci,A.M., Kaufman,T.C. and Kennison,J.A. (1992) *brahma*: a regulator of *Drosophila* homeotic genes structurally related to the yeast transcriptional activator SNF2/SWI2. *Cell*, **68**, 561–572.

Tanaka,S. and Hanafusa,H. (1998) Guanine-nucleotide exchange protein C3G activates JNK1 by a Ras-independent mechanism. JNK1 activation inhibited by kinase negative forms of MLK3 and DLK mixed lineage kinases. *J. Biol. Chem.*, **273**, 1281–1284.

Tanaka,S. *et al*. (1994) C3G, a guanine nucleotide-releasing protein expressed ubiquitously, binds to the Src homology 3 domains of CRK and GRB2/ASH proteins. *Proc. Natl Acad. Sci. USA*, **91**, 3443–3447.

Tanaka,S., Ouchi,T. and Hanafusa,H. (1997) Downstream of Crk adaptor signaling pathway: activation of Jun kinase by v-Crk through the guanine nucleotide exchange protein C3G. *Proc. Natl Acad. Sci. USA*, **94**, 2356–2361.

Teng,K., Lander,H., Fajardo,J.E., Hanafusa,H., Hempstead,B.L. and Birge,R.B. (1995) v-Crk modulation of growth factor-induced PC12 cell differentiation involves the Src homology 2 domain of v-Crk and sustained activation of the Ras/mitogen-activated protein kinase pathway. *J. Biol. Chem.*, **270**, 20677–20685.

Therrien,M., Chang,H.C., Solomon,N.M., Karim,F.D., Wassarman,D.A. and Rubin,G.M. (1995) KSR, a novel protein kinase required for RAS signal transduction. *Cell*, **83**, 879–888.

Tomlinson,A. and Ready,D.F. (1987) Neuronal differentiation in the *Drosophila* ommatidium. *Dev. Biol.*, **120**, 264–275.

van der Meer,S. (1977) Optical clean and permanent whole mount preparation for phase contrast microscopy of cuticular structures of insect larvae. *Drosophila Inf. Serv.*, **52**, 160–161.

Vossler,M.R., Yao,H., York,R.D., Pan,M.G., Rim,C.S. and Stork,P.J. (1997) cAMP activates MAP kinase and Elk-1 through a B-Raf- and Rap1-dependent pathway. *Cell*, **89**, 73–82.

Wassarman,D.A. and Therrien,M. (1997) RAS1-mediated photoreceptor development in *Drosophila. Adv. Dev. Biol.*, **5**, 1–41.

York,R.D., Yao,H., Dilon,T., Ellig,C.L., Eckert,S.P., McCleskey,E.W. and Stork,P.J. (1998) Rap1 mediates sustained MAP kinase activation induced by nerve growth factor. *Nature*, **392**, 622–626.

Yoshida,Y., Kawata,M., Miura,Y., Musha,T., Sasaki,T., Kikuchi,A. and Takai,Y. (1992) Microinjection of smg/rap1/Krev-1 p21 into Swiss 3T3 cells induces DNA synthesis and morphological changes. *Mol. Cell. Biol.*, **12**, 3407–3414.

Received July 28, 1998; revised October 29, 1998;
accepted November 6, 1998